mathematics

MDPI

Article

Asymptotic Antipodal Solutions as the Limit of Elliptic Relative Equilibria for the Two- and n-Body Problems in the Two-Dimensional Conformal Sphere

Rubén Darío Ortiz Ortiz [1,*], Ana Magnolia Marín Ramírez [1] and Ismael Oviedo de Julián [2]

[1] Grupo Ondas, Departamento de Matemáticas, Universidad de Cartagena, Sede San Pablo, Cartagena de Indias 130001, Colombia; amarinr@unicartagena.edu.co
[2] Unidad Azcapotzalco, Departamento de Ciencias Básicas, Universidad Autónoma Metropolitana, Cd. de México 02128, Mexico; iodj@azc.uam.mx
* Correspondence: rortizo@unicartagena.edu.co; Tel.: +57-312-669-1568

Abstract: We consider the two- and n-body problems on the two-dimensional conformal sphere $\mathbb{M}^2_R$, with a radius $R > 0$. We employ an alternative potential free of singularities at antipodal points. We study the limit of relative equilibria under the SO(2) symmetry; we examine the specific conditions under which a pair of positive-mass particles, situated at antipodal points, can maintain a state of relative equilibrium as they traverse along a geodesic. It is identified that, under an appropriate radius–mass relationship, these particles experience an unrestricted and free movement in alignment with the geodesic of the canonical Killing vector field in $\mathbb{M}^2_R$. An even number of bodies with pairwise conjugated positions, arranged in a regular n-gon, all with the same mass m, move freely on a geodesic with suitable velocities, where this geodesic motion behaves like a relative equilibrium. Also, a center of mass formula is included. A relation is found for the relative equilibrium in the two-body problem in the sphere similar to the Snell law.

Keywords: conformal sphere $\mathbb{M}^2_R$; the two-body problem; relative equilibria; antipodal points

MSC: 34D05; 70F15; 53Z05

Citation: Ortiz Ortiz, R.D.; Marín Ramírez, A.M.; Oviedo de Julián, I. Asymptotic Antipodal Solutions as the Limit of Elliptic Relative Equilibria for the Two- and n-Body Problems in the Two-Dimensional Conformal Sphere. *Mathematics* **2024**, *12*, 1025. https://doi.org/10.3390/math12071025

Academic Editor: Ravi P. Agarwal

Received: 29 January 2024
Revised: 17 March 2024
Accepted: 27 March 2024
Published: 29 March 2024

1. Introduction

The study of the n-body problem on curved spaces, especially on spheres, introduces unique challenges and phenomena not present in Euclidean spaces. The work of Borisov et al. [1] provides essential insights into the dynamics of bodies on spaces of constant curvature, foundational for our investigation.

In the realm of celestial mechanics, understanding the intricacies of motion in non-Euclidean geometries is crucial. The research conducted by Ortega-Palencia and Reyes-Victoria [2] and further expanded by Ortega Palencia et al. [3] delves into the n-body problem in spaces of constant positive and negative curvature, offering valuable perspectives that inform our approach.

Our study is also informed by the analysis presented by Diacu et al. [4], which explores the n-body problem in spaces of constant curvature. Their findings provide a broader context for our work, emphasizing the diversity of dynamics that different geometric settings can induce.

The foundational principles laid out by Abraham and Marsden [5] in their seminal work on mechanics provide the theoretical underpinnings for analyzing dynamical systems in a geometric context, essential for our study.

Additionally, the exploration of antipodal equilibria in the two-dimensional sphere by Ortega-Palencia et al. [6] and their further discussion in the arXiv preprint [7] offer important precedents for our study. These works highlight the peculiarities of motion in curved spaces and the significance of the chosen potential in determining the system's behavior.

Through this research, we aim to build on these foundational studies, extending the understanding of the n-body problem in curved spaces and exploring new facets of relative equilibria and their stability. Our work is particularly inspired by the recent developments in the field and seeks to contribute to the ongoing dialogue within the scientific community regarding the dynamics of celestial bodies in non-traditional settings.

We want to point out the possibility of having a relative equilibrium in antipodal points, as stated in [8].

In celestial mechanics with curvature, specifically in the case of a sphere, there are two types of singularities related to the classical cotangent potential [8]. One refers to collisions, while the other refers to antipodal points.

Various researchers, including those cited as [9,10], have explored the behavior of collisions in spaces with non-zero constant curvature by applying classical regularization methods from Newtonian mechanics. Their findings align with those previously obtained in this domain, marking the beginning of investigations into dynamic types.

Additionally, in classical celestial mechanics, an alternative system that helps understand certain movements is studied, such as the planar three-body problem with an attractive potential of $1/r^2$ [11,12]. According to the Lagrange–Jacobi identity, where $\ddot{I} = 4H$, for any solution that is bounded, it is required to possess zero energy and maintain a constant moment of inertia I. This condition holds when the energy at the initial state is zero and its derivative is zero, the solution is bounded, as observed in the Newtonian potential $1/r$.

The work on how to carry out the study of behavior analysis around a geometric singularity, that is, by antipodal points, is just beginning. In this work, a geometric method is proposed to be able to study this type of singularity in the antipodal points for the problem of two bodies in a conformal sphere of dimension two, with one alternative potential that satisfies the Laplace–Beltrami equality [13] and preserves the periodic orbits as the classic cotangent potential in the curved problem.

Our study focuses on the motion of two interacting point particles with masses m_1 and m_2 on the two-dimensional conformal sphere $\mathbb{M}^2_R = \widehat{\mathbb{C}} = \mathbb{C} \cup \{\infty\}$. Consider the complex variable w and its conjugate $\bar{w}$, upon which we define a conformal metric of the form

$$ds^2 = \frac{4R^4}{(R^2 + |w|^2)^2}\, dw\, d\bar{w}, \tag{1}$$

where R is a constant parameter determining the conformal properties of the metric.

We define the corresponding differentiable structure for this space in these coordinates (for more details, refer to [14,15]).

By aligning the vector field within the Lie algebra that corresponds to the associated subgroup with the gravitational field in the cotangent space, we determine the time-dependent algebraic criteria (t) required for solutions to achieve a state of relative equilibrium.

The techniques used in [8,16] are employed in this analysis.

In celestial mechanics on $\mathbb{M}^2_R$, it is common to use the cotangent potential as an extension of the Newtonian potential. This paper presents arguments justifying the introduction of a suitable variant of this potential.

This document is organized as follows:

For an overview of the equations of motion, see Section 2, we have developed a revised potential to tackle the issue, successfully overcoming the challenge of singularities at antipodal points.

We express the equations of motion for the problem in complex coordinates in $\mathbb{M}^2_R$, following the approach used in [8,16].

For insights into elliptic relative equilibria and their properties, consult Section 3: utilizing the newly introduced potential, we formulate the algebraic equations that define the elliptic relative equilibria in the general problem context.

For a detailed exploration of the two-body problem, refer to Section 4: we classify the relative equilibria for the two-body problem, following the approach of Borisov et al. in [17], but considering the new potential.

Regarding the analysis of antipodal points, see Section 5: for any antipodal pair of points in $\mathbb{M}^2_R$, we successfully derive limiting solutions by applying a regularized version of the original equations of motion.

2. Dynamics Formulation and Conditions for Equilibrium

As discussed in [8], utilizing the stereographic projection method, the authors formulate the motion equations pertinent to this problem. This involves projecting the sphere (with a radius of R) from its embedding in $\mathbb{R}^3$ onto the complex plane $\mathbb{C}$, which utilizes the specified metric (1).

In Ref. [5], the classical motion equations for particles with positive masses m_k, $k = 1, \ldots, n$ are discussed, situated within a Riemannian or semi-Riemannian manifold characterized by coordinates $x^k, k = 1, \ldots, N$, endowed with a metric (g_{ij}) and an associated connection Γ^i_{jk}. The connection here, specifically the Levi-Civita connection, is not arbitrary. It is determined by the specified metric (1) through the Christoffel symbols, which are uniquely defined by the metric to ensure the connection is torsion-free and metric-compatible.

Replacing the Levi-Civita connection with an arbitrary one could lead to a different set of Christoffel symbols, altering the motion equations and, consequently, the particles' trajectories and equilibrium states. Such changes would reflect a fundamental shift in the geometric structure of the space in which the particles are moving.

These particles move under the influence of a pairwise-acting potential U.

Theorem 1. *Consider a system of n particles with positive masses m_k, $k = 1, \ldots, n$, situated within a Riemannian or semi-Riemannian manifold characterized by coordinates $x^k, k = 1, \ldots, N$, and endowed with a metric (g_{ij}) as specified in (1) and an associated Levi-Civita connection Γ^i_{jk}. The equations of motion for these particles under the influence of a pairwise-acting potential U are given by*

$$\frac{D\dot{x}^i}{dt} = \ddot{x}^i + \sum_{l,j} \Gamma^i_{lj} \dot{x}^l \dot{x}^j = \sum_k m_k g^{ik} \frac{\partial U}{\partial x^k}, \tag{2}$$

where $i = 1, 2, \ldots, N$. If the potential U is constant across a connected domain, the particle trajectories align with the geodesics of the manifold defined by the metric (1).

Proof. Given the manifold's metric (g_{ij}) specified in (1) and the associated Levi-Civita connection Γ^i_{jk}, the covariant derivative $\frac{D\dot{x}^i}{dt}$ accounts for the curvature dictated by (1) and ensures that the acceleration $\ddot{x}^i$ is defined in a coordinate-independent manner. The equation of motion incorporates both the intrinsic geometry of the manifold, represented by the Christoffel symbols Γ^i_{lj}, and the external force derived from the potential U. When U is constant, the term $\sum_k m_k g^{ik} \frac{\partial U}{\partial x^k}$ vanishes, indicating that the particles' acceleration is solely dictated by the manifold's geometry as defined by (1), thus aligning their trajectories with geodesics. □

Remark 1. *It is noted that in Equation (2) the covariant derivative of $\dot{x}^i$ is represented on the left-hand side, whereas the gradient of the potential within the specified metric is depicted on the right-hand side. Should the potential remain constant, particle trajectories align with geodesics. If a set of particles moves along a geodesic solution curve, then the right-hand side of Equation (2) vanishes, such that the solution of the potential is constant on one connected domain.*

In this section, we introduce the motion equations for the n-body problem within the conformal sphere denoted as $\mathbb{M}^2_R$.

2.1. Introducing the Novel Potential

Exploring the n-body problem on the sphere, we reference a potential frequently encountered in contemporary research, expressed as follows:

$$U(\theta) = \cot(\theta), \tag{3}$$

in which θ is the angle at the center of the sphere, delineated by the position vectors of the particles. This potential is attractive because $\frac{dU}{d\theta}(\theta) = -\csc^2(\theta) < 0, 0 < \theta < \pi$.

Here, we introduce a slight modification to the potential (3) and define it as the new potential:

$$U(\theta) = \cot\left(\frac{\theta}{2}\right), \tag{4}$$

which remains attractive over the entire interval $(0, 2\pi)$.

Theorem 2. *Consider a pair of particles with masses m_k and m_j positioned at locations A_k and A_j on the sphere $\mathbb{S}^2_R$. If w_k and w_j are their respective stereographic projections onto $\mathbb{M}^2_R$, then the potential U^{kj}_R experienced by the particles is given by*

$$U^{kj}_R = m_k m_j \frac{1}{R} \cot\left(\frac{d_{kj}}{2R}\right) = m_k m_j \frac{|R^2 + w_k \bar{w}_j|}{R^2 |w_k - w_j|}. \tag{5}$$

Proof. Given the particles at A_k and A_j on $\mathbb{S}^2_R$, the geodesic distance d_{kj} between them is related to the angle θ_{kj} at the origin by $d_{kj} = R\theta_{kj}$. From the trigonometric identity on the sphere, we have

$$\cos(\theta_{kj}) = \frac{A_k \cdot A_j}{R^2}.$$

Applying the law of cosines for spherical trigonometry gives us

$$\cot\left(\frac{d_{kj}}{2R}\right) = \sqrt{\frac{R^2 + A_k \cdot A_j}{R^2 - A_k \cdot A_j}}.$$

Using the stereographic projection, the dot product $A_k \cdot A_j$ in terms of w_k and w_j is

$$A_k \cdot A_j = R^2 \left(\frac{2R^2(w_k \bar{w}_j + \bar{w}_k w_j) + (R^2 - |w_k|^2)(R^2 - |w_j|^2)}{(R^2 + |w_k|^2)(R^2 + |w_j|^2)} \right).$$

Substituting this into the cotangent expression and simplifying yields the potential experienced by the particles as

$$U^{kj}_R = m_k m_j \frac{|R^2 + w_k \bar{w}_j|}{R^2 |w_k - w_j|},$$

which completes the proof. □

2.2. Equations of Motion

Designate $\mathbf{w} \in (\mathbb{M}^2_R)^n$ as the collective position vector for n particles, each with mass $m_i > 0$, situated at points w_i for $i = 1, 2, \ldots, n$, within the space $\mathbb{M}^2_R$.

The set of singularities within $\mathbb{M}^2_R$ for the n-body problem, as defined by the cotangent relation, comprises the solutions to the equation $w_j - w_k = 0$. Proceeding from this point, the singular set is identified as

$$\Delta(C) = \bigcup_{kj} \Delta(C)_{kj}, \tag{6}$$

where

$$\Delta(C)_{kj} = \left\{ \mathbf{w} \in (\mathbb{M}_R^2)^n \mid w_k = w_j,\, k \neq j \right\} \tag{7}$$

represents instances of mutual collisions between particles having masses m_j and m_k.

Theorem 3 (Dynamics of n-Body Problem in $\mathbb{M}_R^2$)**.** *Consider a set of n point particles with masses $m_i > 0$ situated at points w_i within the Riemannian manifold $\mathbb{M}_R^2$, where $\mathbf{w} \in (\mathbb{M}_R^2)^n$ represents the collective position vector of these particles. The dynamics of each particle is governed by the following equation:*

$$\ddot{w}_k - \frac{2\bar{w}_k \dot{w}_k^2}{R^2 + |w_k|^2} = \frac{(R^2 + |w_k|^2)^2}{4R^6} \sum_{j \neq k}^{n} m_j \frac{(w_j - w_k)(R^2 + \bar{w}_j w_k)(R^2 + |w_j|^2)}{|w_j - w_k|^3 |R^2 + \bar{w}_j w_k|}, \tag{8}$$

for $k = 1, 2, \ldots, n$.

Proof. The proof follows from integrating the geodesic equations for $\mathbb{M}_R^2$ and the gradients computed from the potential U_R, as detailed in the equations provided, into the dynamics defined by the Vlasov–Poisson equations. The resulting second-order complex ordinary differential equations dictate the motion of the particles, ensuring that the trajectories remain within the specified domain, avoiding the singular set $\Delta(C)$. □

Corollary 1 (Singular Set and Binary Collisions in $\mathbb{M}_R^2$)**.** *In the space $\mathbb{M}_R^2$, the singular set $\Delta(C)$ for the n-body problem consists solely of points satisfying $w_j - w_k = 0$ for any pair of particles j, k where $j \neq k$, indicating binary collisions. Antipodal points satisfying $R^2 + w_j \bar{w}_k = 0$ are not considered part of the singular set in terms of the equations of motion.*

Proof. The characterization of the singular set stems from the definition of mutual collisions between particles, which are the only points where the potential U_R becomes undefined or singular. The exclusion of antipodal points from the singular set is due to the specific structure of the potential and the forces it dictates, which remain well defined for antipodal configurations. □

3. Elliptic Relative Equilibria

The group $\mathrm{SU}(2)$ is given by the Lie algebra $\mathrm{su}(2)$ generated by three matrices; for our purposes we only work with the complex matrix:

Theorem 4. *In the two-dimensional conformal sphere $\mathbb{S}_R^2$, the one-parameter subgroup generated by $\exp(tX)$, where $X = \begin{pmatrix} i & 0 \\ 0 & -i \end{pmatrix}$, induces a family of elliptic Möbius transformations. For any point w in the disk $\mathbb{D}_R^2$ of radius R in the complex plane, the trajectory under this transformation is a circular path given by $f(t, w) = e^{2it}w$, representing a rotation around the z-axis in $\mathbb{R}^3$. This circular motion corresponds to the differential equation $\dot{w} = 2iw$, signifying the dynamical system's relative equilibrium state.*

Proof. The exponential mapping applied to the line $\{tX : t \in \mathbb{R}\}$ yields the one-parameter subgroup $\exp(tX) = \begin{pmatrix} e^{it} & 0 \\ 0 & e^{-it} \end{pmatrix}$. The modulus of the off-diagonal elements, $|e^{\pm it}|$, is equal to 1, characterizing elliptic transformations since $e^{\pm it} \neq \pm 1$ for $t \in \mathbb{R}$. The action of this subgroup on a point w in $\mathbb{D}_R^2$ is described by the Möbius transformation $f(t, w) = e^{2it}w$, which geometrically corresponds to a rotation around the z-axis. The trajectory of w under this transformation is a circular path in $\mathbb{D}_R^2$, aligning with the differential equation $\dot{w} = 2iw$. This demonstrates that the system is in a state of relative equilibrium, as the trajectories are circular paths dictated by the subgroup's rotational action. □

The trajectories generated by the one-parameter subgroup $\exp(tX)$ in $\mathbb{C}$, along with the circular paths on the two-dimensional sphere situated in $\mathbb{R}^3$, are illustrated in Figures 1 and 2.

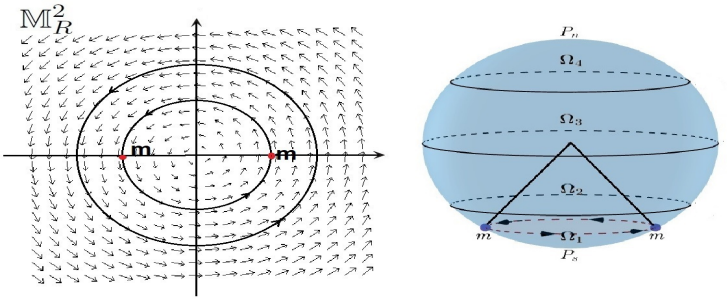

Figure 1. Isosceles solutions.

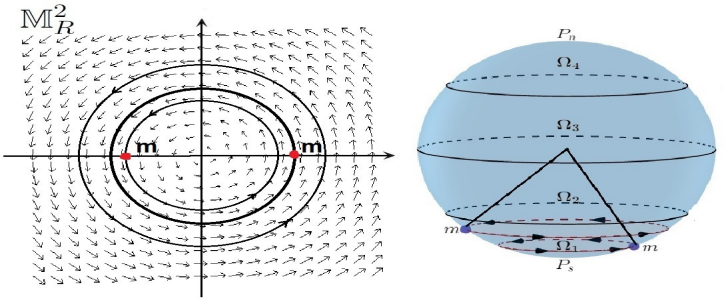

Figure 2. Right-angled solutions.

Now, we can start our analysis of the so-called *solutions of elliptic relative equilibria*, derived from the influence of the canonical one-dimensional parametric subgroup within $\mathrm{SU}(2)$, corresponding to the differential equation $\dot{w}_k = 2iw_k$. There is a study of the action of the subgroup in [2,8,17] for the classic cotangent potential.

Definition 1. *An elliptic relative equilibrium for the n-body problem in $\mathbb{M}^2_R$ is a solution $\mathbf{w}(t) = (w_1(t), w_2(t), \cdots, w_n(t))$ of the equations of motion (8) that is invariant under the Killing vector field $\dot{w}_k = 2i\, w_k$.*

We now present the following lemma:

Theorem 5. *In the case of n point particles, each with positive masses m_k, $k = 1, \ldots, n$, moving within $\mathbb{M}^2_R$, the requisite condition for $\mathbf{w}(t)$ to qualify as an elliptic relative equilibrium solution under (8) is encapsulated by the subsequent rational complex functional equations, which are time-dependent:*

$$16R^6 \frac{(R^2 - |w_k|^2)w_k}{(R^2 + |w_k|^2)^3} = \sum_{j=1, j\neq k}^{n} \frac{m_j(|w_j|^2 + R^2)(R^2 + \bar{w}_j w_k)(w_j - w_k)}{|R^2 + \bar{w}_j w_k||w_j - w_k|^3} \tag{9}$$

where the velocity at each point is given by $\dot{w}_k = 2iw_k$, where w_k represents the value of the k-th component of the vector $\mathbf{w}$.

Proof. Through direct calculations, we find that from equation $\dot{w}_k = 2i\, w_k$, we have $\ddot{w}_k = -4\, w_k$. Substituting this into Equation (8) yields Equality (9). □

The subsequent finding outlines prerequisites for the particles' initial placements to yield an elliptic relative equilibrium solution for Equation (9). These solutions depend on the fixed points and their velocities.

Corollary 2. *In line with Theorem 5, the initial positions $w_{k,0}$, $k = 1, \ldots, n$ fulfill a necessary and sufficient criterion to produce an elliptic solution for the system (8), which remains invariant under the Killing vector field $\dot{w}k = 2iw_k$, through this set of algebraic equations:*

$$16R^6 \frac{(R^2 - |w_{k,0}|^2)w_{k,0}}{(R^2 + |w_{k,0}|^2)^3} = \sum_{j \neq k}^{n} \frac{m_j(w_{j,0} - w_{k,0})(R^2 + \bar{w}_{j,0}w_{k,0})(R^2 + |w_{j,0}|^2)}{|w_{j,0} - w_{k,0}|^3 |R^2 + \bar{w}_{j,0}w_{k,0}|}. \tag{10}$$

Furthermore, the required velocity for each particle is determined by the equation $\dot{w}_{k,0} = 2iw_{k,0}$, where k ranges from 1 to n, where $w_{k,0}$ represents the initial value of the k-th component of the vector $\mathbf{w}$.

Proof. Take $w_k = w_k(t) = e^{2it}w_{k,0}$ to represent the impact of the Killing vector field $\dot{w}_k = 2iw_k$ at the initial position $w_{k,0}$, corresponding to a velocity of $\dot{w}_{k,0} = 2iw_{k,0}$. By applying a multiplication of Equation (10) with e^{2it} and incorporating the identity $\bar{w}_j(t)w_k(t) = \bar{w}_{j,0}e^{-2it}w_{k,0}e^{2it} = \bar{w}_{j,0}w_{k,0}$, the resultant system is derived:

$$16\,R^6 \frac{(R^2 - |w_k|^2)w_k}{(R^2 + |w_k|^2)^3} = \sum_{j=1, j \neq k}^{n} \frac{m_j\,(w_j - w_k)(R^2 + \bar{w}_j w_k)(R^2 + |w_j|^2)}{|w_j - w_k|^3\,|R^2 + \bar{w}_j w_k|}.$$

This demonstrates that $w_k(t)$ serves as a solution to (9). To establish the reverse argument, one simply sets $t = 0$ within the framework of (9), thereby concluding the corollary's proof. □

References [2,8] provide illustrative examples of the two- and three-body problems situated on the conformal sphere $\mathbb{M}^2_R$ with the classical cotangent potential.

4. Equilibria States in the Two-Body Problem Context

In the following segment, it is shown that relative equilibria exist in the context of the two-body problem, specifically when employing potential (5), where the bodies are in motion on the same circle or on two different circles. These results are consistent with the findings in [1,2,8] for the classical cotangent potential.

Theorem 6. *For the values of initial condition positions $w_{1,0} = \alpha$ and $w_{2,0} = \beta$ (with $0 < \alpha, \beta < R$), for the two-body problem with equal masses on the conformal sphere $\mathbb{M}^2_R$, the system (10) yields only two types of relative equilibrium solutions:*

1. *Under the condition $\frac{3\sqrt{3}R^3}{2} \geq m$, the particles position themselves diametrically opposite on the same circle, with $-\beta = \alpha$, termed as isosceles solutions (refer to Figure 1).*
2. *Given the condition $2R^3 \geq m$, the particles occupy positions on separate circles, with $\beta = R\frac{(\alpha - R)}{\alpha + R}$, creating a right angle, known as right-angled solutions (refer to Figure 2).*
3. *Both types of relative equilibria coincide for the value of $\alpha = (\sqrt{2} - 1)R$.*

The solutions for β are in the interval $(-R, 0)$.

Proof. Firstly, in positions $w_{1,0}$ and $w_{2,0}$, we note that the system (10) for the two-body problem can be expressed as the following algebraic system:

$$\begin{aligned} 16R^6 \frac{(|w_{1,0}|^2 - R^2)w_{1,0}}{(R^2 + |w_{1,0}|^2)^3} &= m_2 \frac{(w_{2,0} - w_{1,0})(R^2 + \bar{w}_{2,0}w_{1,0})(R^2 + |w_{2,0}|^2)}{|w_{2,0} - w_{1,0}|^3 |R^2 + w_{1,0}\bar{w}_{2,0}|}, \\ 16R^6 \frac{(|w_{2,0}|^2 - R^2)w_{2,0}}{(R^2 + |w_{2,0}|^2)^3} &= m_1 \frac{(w_{1,0} - w_{2,0})(R^2 + \bar{w}_{1,0}w_{2,0})(R^2 + |w_{1,0}|^2)}{|w_{1,0} - w_{2,0}|^3 |R^2 + \bar{w}_{1,0}w_{2,0}|}. \end{aligned} \tag{11}$$

From Corollary 2, by performing a suitable rotation, a condition both necessary and sufficient for the presence of invariant elliptic solutions influenced by the Killing vector field $\dot{w}_k = 2iw_k$ dictates that the initial positions $w_{1,0} = \alpha$ and $w_{2,0} = \beta$ (where $0 < \alpha, \beta < R$)

must conform to system (11). Since $R^2 + \beta\alpha > 0$, when substituted into the system, it becomes

$$\begin{aligned} 16R^6\frac{(\alpha^2-R^2)\alpha}{(\alpha^2+R^2)^3} &= m_2\frac{(\beta-\alpha)(\beta\alpha+R^2)(\beta^2+R^2)}{|\beta-\alpha|^3|R^2+\alpha\beta|} = m_2\frac{(\beta-\alpha)(R^2+\beta^2)}{|\beta-\alpha|^3}, \\ 16R^6\frac{(\beta^2-R^2)\beta}{(R^2+\beta^2)^3} &= m_1\frac{(\alpha-\beta)(R^2+\alpha\beta)(R^2+\alpha^2)}{|\alpha-\beta|^3|R^2+\alpha\beta|} = m_1\frac{(\alpha-\beta)(\alpha^2+R^2)}{|\alpha-\beta|^3}. \end{aligned} \quad (12)$$

By equalizing the right- and left-hand sides of (12) and replacing $w_{1,0} = \alpha$, $w_{2,0} = \beta$, the following relation is derived:

$$m_1(\alpha-R)(\alpha+R)(R^2+\beta^2)^2\alpha + m_2(\beta-R)(\beta+R)(R^2+\alpha^2)^2\beta = 0. \quad (13)$$

For $m = m_1 = m_2$, the solutions to the system outlined in (12), derived from Equation (13), are as follows:

$$-\beta = \alpha, \qquad \beta = R\frac{(\alpha-R)}{\alpha+R}, \qquad \beta = R^2\frac{1}{\alpha}, \qquad \beta = -R\frac{(\alpha+R)}{\alpha-R},$$

which is readily apparent.

1. For the initial scenario where $-\beta = \alpha$, the result is the isosceles configurations, and by substituting it into any of the equations in system (12), we obtain the relation

$$\frac{R^6(R^2-\alpha^2)\alpha^3}{(R^2+\alpha^2)^4} = \frac{m}{64}.$$

We consider the function

$$F(\alpha) = \frac{R^6(R^2-\alpha^2)\alpha^3}{(R^2+\alpha^2)^4},$$

defined in the interval $[0, R]$. It has a maximum value of $\frac{3\sqrt{3}R^3}{128}$ at the critical point $\frac{\sqrt{3}R}{3}$.

A simple analysis shows that there are isosceles solutions for this problem if $\frac{3\sqrt{3}R^3}{128} \geq \frac{m}{64}$, which proves the first item.

2. In the subsequent case, consider ℓ as the geodesic distance between α and $\beta = R\frac{(\alpha-R)}{\alpha+R}$. First, let us establish that β is always smaller than α within the interval $\left[R\frac{(\alpha-R)}{\alpha+R}, \alpha\right]$. To determine which is smaller in the interval $\left[R\frac{(\alpha-R)}{\alpha+R}, \alpha\right]$, we compare $R\frac{(\alpha-R)}{\alpha+R}$ with α.

- If $\alpha = R$, then $R\frac{(\alpha-R)}{\alpha+R} = 0$, which is clearly smaller than α since $\alpha = R > 0$.
- If $\alpha < R$, then $\alpha - R < 0$. This implies that $R\frac{(\alpha-R)}{\alpha+R}$ is negative, and therefore, smaller than α, which is positive.
- We analyze the difference $\alpha - R\frac{(\alpha-R)}{\alpha+R}$:

$$\begin{aligned} \alpha - R\frac{(\alpha-R)}{\alpha+R} &= \frac{\alpha(\alpha+R)-R(\alpha-R)}{\alpha+R} \\ &= \frac{\alpha^2+\alpha R-R\alpha+R^2}{\alpha+R} \\ &= \frac{\alpha^2+R^2}{\alpha+R}. \end{aligned}$$

Since $\alpha^2 + R^2 > 0$ and $\alpha + R > 0$ for $\alpha, R > 0$, the difference is positive, indicating that α is greater than $R\frac{(\alpha-R)}{\alpha+R}$.

Therefore, in all cases within the interval $\left[R\frac{(\alpha-R)}{\alpha+R}, \alpha\right]$, the point $R\frac{(\alpha-R)}{\alpha+R}$ is always smaller than α.

By defining the arc Γ that connects points β and α through a parametrization given by

$$x(t) = t, \tag{14}$$

$$y(t) = 0, \tag{15}$$

over the interval $\left[R\frac{(\alpha-R)}{\alpha+R}, \alpha\right]$, the geodesic distance ℓ can be calculated as follows:

$$\begin{aligned} \ell &= \int_\Gamma d\ell = 2R^2 \int_{R\frac{(\alpha-R)}{\alpha+R}}^{\alpha} \frac{dt}{t^2+R^2} && (16)\\ &= 2R\left[\arctan\left(\frac{\alpha}{R}\right) - \arctan\left(\frac{R(\alpha-R)}{R(\alpha+R)}\right)\right] && (17)\\ &= 2R\arctan\left(\frac{\frac{\alpha}{R} - \frac{\alpha-R}{\alpha+R}}{1+\frac{\alpha}{R}\frac{\alpha-R}{\alpha+R}}\right) && (18)\\ &= 2R\arctan(1) = \frac{\pi R}{2}. && (19) \end{aligned}$$

Now, let us consider the asymptotic behavior of ℓ as α approaches R and 0:

1. As α approaches R, the geodesic distance ℓ should theoretically approach 0 as the two points converge.
2. As α approaches 0, the point β approaches $-R$, and the geodesic distance ℓ should approach the maximum possible value on the circle, which is πR, corresponding to half the circumference of the circle of radius R.

This analysis provides a deeper understanding of the geometric configuration of the system and the behavior of the geodesic distance under different conditions.

This delineates the process and calculation of length ℓ for the specified path Γ within the two-dimensional manifold $\mathbb{M}^2_R$.

Conversely, it is established that $\ell = \theta R$, with θ denoting the angle between the specified points in $\mathbb{M}^2_R$. Consequently, $\theta = \frac{\pi}{2}$, classifying the solution as right-angled.

In this case, by substituting $\beta = \frac{R(\alpha-R)}{\alpha+R}$ into any of the equations in the system (12), we obtain the relation

$$\frac{R^4(R^2-\alpha^2)\alpha}{(R^2+\alpha^2)^2} = \frac{m}{8}.$$

We consider the function

$$G(\alpha) = \frac{R^4(R^2-\alpha^2)\alpha}{(R^2+\alpha^2)^2},$$

defined in the interval $[0, R]$. It has a maximum value of $\frac{R^3}{4}$ at the critical point $(\sqrt{2}-1)R$. Once again, a simple analysis shows that there are right-angled solutions for this problem if $\frac{R^3}{4} \geq \frac{m}{8}$, which proves the second item.

This concludes the proof. □

In [1], in theorem 4.3 there is a discussion about the stability of the solutions obtained.

In this theorem, we establish a connection between the relative equilibria for the two-body problem and Snell's law of geometric optics.

Theorem 7. *If two particles in the two-body problem are in relative equilibrium and the given substitution conditions are met, then the relationship between their masses and positions is analogous to Snell's law, with the particularity that the "indices of refraction" are the masses and the "angles of refraction" are related to the positions of the particles.*

Proof. Consider the following equation derived from the polynomial equation for the two-body problem (see Equation (13)):

$$\frac{m_1\alpha(\alpha^2 - R^2)}{(\alpha^2 + R^2)^2} = -\frac{m_2\beta(\beta^2 - R^2)}{(\beta^2 + R^2)^2} \tag{20}$$

Here, $\tan(\theta_1) = \frac{\alpha}{R}$ and $\tan(\theta_2) = \frac{\beta}{R}$. Let us substitute $\alpha = R\tan(\theta_1)$ and $\beta = R\tan(\theta_2)$ into Equation (20):

$$\frac{m_1 R\tan(\theta_1)(R^2\tan^2(\theta_1) - R^2)}{(R^2\tan^2(\theta_1) + R^2)^2} = -\frac{m_2 R\tan(\theta_2)(R^2\tan^2(\theta_2) - R^2)}{(R^2\tan^2(\theta_2) + R^2)^2}$$

Simplifying the equation, we obtain

$$m_1\tan(\theta_1)(\tan^2(\theta_1) - 1) = -m_2\tan(\theta_2)(\tan^2(\theta_2) - 1)$$

Using the trigonometric identity $\tan^2(\theta) - 1 = -\cos(2\theta)$, we can rewrite the equation as

$$m_1\tan(\theta_1)\cos(2\theta_1) = -m_2\tan(\theta_2)\cos(2\theta_2)$$

Now, using the double-angle formula $\sin(2\theta) = 2\sin(\theta)\cos(\theta)$, we can express $\tan(\theta)\cos(2\theta)$ in terms of $\sin(4\theta)$:

$$m_1\sin(4\theta_1) = -m_2\sin(4\theta_2)$$

This relationship is analogous to Snell's law, where the masses act as indices of refraction and the angles are related to the positions of the particles, thus proving the theorem. □

5. Exploring Antipodal Solutions: Approaching through the Lens of Relative Equilibria

Within this segment, our focus shifts to the examination of antipodal solutions that emerge in the context of the two-body problem when considering scenarios involving bodies of identical mass.

Antipodal Solutions as a Limit of Relative Equilibria for Equal Masses

According to Theorem 6, there are two types of relative equilibria for equal masses, and each type gives rise to a different solution as α approaches R.

Corollary 3. *In the context of right-angled relative equilibria, as α approaches R a state of equilibrium for the system is achieved. In this state, one particle is positioned at the origin of coordinates, while the other follows a geodesic circular path with a radius of $|w| = R$, moving at a velocity of $\dot{w} = 2iw$.*

Proof. The assertion is derived from the observation that as α tends towards R, β converges to 0, as demonstrated by

$$\lim_{\alpha\to R}\beta = \lim_{\alpha\to R}\frac{R(\alpha - R)}{\alpha + R} = 0,$$

as α nears R. □

Next, we examine the scenarios involving conjugate (antipodal) points within the two-body problem, considering them as limiting cases of isosceles configurations. This analysis becomes particularly relevant when α nears R and the criterion for the radius–mass relationship, $\frac{3\sqrt{3}R^3}{2} \geq m$, is met.

We present the following result, which demonstrates that the family of relative equilibria converges to the geodesic circle (equator), acting as a unified relative equilibrium since it remains invariant under the canonical Killing vector field. However, while it does

not serve as a solution to the overarching system (8), it constitutes a geodesic within $\mathbb{M}^2_R$, where the potential exerted along this trajectory is nullified.

Nevertheless, a solution to the regularized system derived from (8) exists on this geodesic.

Theorem 8. *In the limit as α approaches R, the family of isosceles relative equilibria becomes an equilibrium with equal masses, where the particles are located at antipodal points. These particles move along the geodesic circle where $|w| = R$, possessing a velocity given by $\dot{w}(t) = 2iw(t)$, and behave as a single (limit) relative equilibrium.*

Proof. We note that for the two-body problem involving equal masses, the potential is described as follows:

$$U_R(\mathbf{w}, \bar{\mathbf{w}}) = \frac{m^2 \left| R^2 + w_2 \bar{w}_1 \right|}{R^2 |w_2 - w_1|}. \tag{21}$$

Let $w_1(t) = \alpha e^{2it}$ and $w_2(t) = -\alpha e^{2it}$ constitute the elements of the relative equilibrium:

$$w(t) = (\alpha e^{2it}, -\alpha e^{2it}).$$

Substituting these values into Equation (21), we obtain

$$\begin{aligned} U_R(\mathbf{w}, \bar{\mathbf{w}}) &= \frac{m^2}{R^2} \frac{|R^2 + (-\alpha e^{2it})(\alpha e^{-2it})|}{|2\alpha e^{2it}|} \\ &= \frac{m^2}{2\alpha} \frac{(R^2 - \alpha^2)}{R^2}. \end{aligned}$$

This shows that the potential along the family of relative equilibria decreases and converges to zero as α approaches R.

If we denote $z_1(t) = Re^{2it}$ and $z_2(t) = -Re^{2it}$ as the components of the function:

$$z(t) = (z_1(t), z_2(t)) = (Re^{2it}, -Re^{2it}), \tag{22}$$

where each coordinate maps out the geodesic circle with radius R, moving at a velocity of $\dot{z}(t) = 2iz(t)$, then

$$\lim_{\alpha \to R} w(t) = \lim_{\alpha \to R} (\alpha e^{2it}, -\alpha e^{2it}) = (Re^{2it}, -Re^{2it}) = z(t).$$

Given the potential's continuity and that conjugate points cease to be singularities for the potential, it follows that

$$\begin{aligned} U_R(\mathbf{z}, \bar{\mathbf{z}}) &= \lim_{\alpha \to R} U_R(\mathbf{w}, \bar{\mathbf{w}}) \\ &= \lim_{\alpha \to R} \left(\frac{m^2}{2\alpha R^2} \left(R^2 - \alpha^2 \right) \right) = 0. \end{aligned}$$

This illustrates that the potential becomes null along the geodesic circle (22).

Inserting $\beta = -R \quad \text{and} \quad \alpha = R$ into Equation (13) confirms it as a solution to both that equation and the regularized system derived from the relative equilibria condition system (12), specified as follows:

$$16R^6\alpha\frac{(\alpha^2-R^2)}{(R^2+\alpha^2)^3}\,|R^2+\alpha\beta| = m_2\frac{(\beta-\alpha)(R^2+\beta\alpha)(R^2+\beta^2)}{|\beta-\alpha|^3},$$
$$16R^6\beta\frac{(\beta^2-R^2)}{(R^2+\beta^2)^3}\,|R^2+\alpha\beta| = m_1\frac{(\alpha-\beta)(R^2+\alpha\beta)(R^2+\alpha^2)}{|\alpha-\beta|^3}.$$

Clearly, the function (22) does not resolve the general system (8). Nonetheless, through straightforward substitution it fulfills the criteria of the regularized system derived from (8) by circumventing singularities, including those arising from conjugate antipodal points:

$$\left(\ddot{\bar{w}}_1-\frac{2\bar{w}_1\dot{\bar{w}}_1^2}{R^2+|w_1|^2}\right)\frac{|R^2+\bar{w}_2w_1|}{(R^2+|w_1|^2)^2} = m_2\frac{(w_2-w_1)(R^2+\bar{w}_2w_1)(R^2+|w_2|^2)}{4R^6|w_2-w_1|^3},$$
$$\left(\ddot{\bar{w}}_2-\frac{2\bar{w}_2\dot{\bar{w}}_2^2}{R^2+|w_2|^2}\right)\frac{|R^2+\bar{w}_1w_2|}{(R^2+|w_2|^2)^2} = m_1\frac{(w_1-w_2)(R^2+\bar{w}_1w_2)(R^2+|w_1|^2)}{4R^6|w_1-w_2|^3}.$$

This concludes the proof. □

Corollary 4. *In the limit as particles approach antipodal positions on the sphere, the interaction potential between them tends to zero, and the particles behave as if they are in a relative equilibrium state without mutual influence. This occurs along the geodesic circle where $|w| = R$, with the particles possessing a velocity given by $\dot{w}(t) = 2iw(t)$.*

Proof. From the theorem's proof, we note that as α approaches R, the potential $U_R(\mathbf{w}, \bar{\mathbf{w}})$ converges to zero. This indicates that the interaction force between the particles diminishes and vanishes in the limit. Therefore, when the particles are at antipodal points, they move along the geodesic circle without influencing each other, maintaining a constant velocity $\dot{w}(t) = 2iw(t)$, characteristic of a relative equilibrium in the system. □

Corollary 5. *Any pair of antipodal point particles with equal masses, satisfying the condition on the radius–mass relation $\frac{3\sqrt{3}R^3}{2} \geq m$, can move freely along the geodesic associated with the (finite) direction of the Killing vector field in the two-dimensional sphere $\mathbb{M}^2_R$.*

Proof. Given system (12) and polynomial Equation (13), we analyze the case where $m = m_1 = m_2$. For the solutions outlined, we particularly focus on the scenario where $-\beta = \alpha$. Substituting this into the system yields the relation

$$\frac{R^6(R^2-\alpha^2)\alpha^3}{(R^2+\alpha^2)^4} = \frac{m}{64}. \tag{23}$$

Consider the function $F(\alpha) = \frac{R^6(R^2-\alpha^2)\alpha^3}{(R^2+\alpha^2)^4}$ defined in the interval $[0, R]$. It reaches a maximum at $\alpha = \frac{\sqrt{3}R}{3}$ with a value of $\frac{3\sqrt{3}R^3}{128}$.

The condition for the existence of solutions is $\frac{3\sqrt{3}R^3}{128} \geq \frac{m}{64}$. Since this aligns with the condition provided in the corollary, $\frac{3\sqrt{3}R^3}{2} \geq m$, the statement is proven for the specified configuration. □

6. Relative Equilibrium for the n-Body Problem

Corollary 6. *An even number of point particles with pairwise conjugated positions $w_j(t)$, arranged in a regular n-gon and with equal masses, move freely on a geodesic with velocities $\dot{w}_j = 2iw_j(t)$. This geodesic movement behaves as a relative equilibrium.*

Proof. We observe that from Remark 1, a necessary and sufficient condition for a set of n particles with masses m_k to move along a geodesic solution curve, where the right-hand side of Equation (2) vanishes along such a solution, is given by the system of equations, we can approximate $R^2 + \bar{w}_j w_k$ by $R^2 + \bar{w}_j w_k + \epsilon$ for some sufficiently small ϵ:

$$0 = \sum_{j<k}^{n} m_j \frac{(w_j - w_k)(R^2 + \bar{w}_j w_k + \epsilon)(R^2 + |w_j|^2)}{|w_j - w_k|^3 |R^2 + \bar{w}_j w_k + \epsilon|} = \sum_{j<k}^{n} m_j \frac{(w_j - w_k)(R^2 + \bar{w}_j w_k + \epsilon)}{|w_j - w_k|^3 |R^2 + \bar{w}_j w_k + \epsilon|}, \tag{24}$$

where the sum is taken over $j, k = 1, 2, \cdots, n$.

Therefore, for the n-body problem with equal mass particles moving along a geodesic circle, we have the equality

$$0 = \sum_{j<k}^{n} \frac{(w_j - w_k)(R^2 + \bar{w}_j w_k + \epsilon)}{|w_j - w_k|^3 |R^2 + \bar{w}_j w_k + \epsilon|}. \tag{25}$$

Using the same method of applying a rotation for conjugate points into the line as in Theorem 8 for an n-even number of equal masses arranged in a regular n-gon along a geodesic, and considering that the acting forces for any elements w_k and w_j cancel in pairs, we obtain the equation

$$\frac{(w_j - w_k)(R^2 + \bar{w}_j w_k + \epsilon)}{|w_j - w_k|^3 |R^2 + \bar{w}_k w_j + \epsilon|} + \frac{(w_k - w_j)(R^2 + \bar{w}_k w_j + \epsilon)}{|w_k - w_j|^3 |R^2 + \bar{w}_j w_k + \epsilon|} = 0. \tag{26}$$

This leads us to the result, which complements the one obtained in Theorem 5 in [4] for an odd number of particles with equal masses moving along a geodesic. □

Remark 2. *In remark 3 in [4], the authors parameterize the relative equilibria using a relation between angular velocity, the equal masses of the bodies, and their positions on the sphere. This leads to the observation that the velocity approaches infinity as the particles tend to the equator. However, we believe it is not physically possible to speak of this scenario in our universe for the following reasons:*

1. *When the angular light velocity $\dot{w}(0) = \pm 2i\,\alpha_\infty$ is reached for the initial condition $w(0) = \pm\,\alpha_\infty$, the masses corresponded to elementary particles and such quantities vanish.*
2. *The annular region*

$$\Omega = \{w \in \mathbb{M}^2_R \mid \alpha_\infty < |w| < R + \alpha_\infty\}$$

containing the equator $|w| = R$ does not admit any other real relative equilibria for this problem.

7. Center of Mass on a Two-Dimensional Sphere

In the study presented in [6], the concept of the center of mass for particles on a spherical surface $\mathbb{S}^2_R$ was explored. Here, we formalize this concept into a theorem and provide a demonstration of the underlying principle.

Theorem 9. *Given two particles on $\mathbb{S}^2_R$, it is always possible to map them to the equator determined by their intersection with the xy-plane using an isometry, which is a composition of two rotations. This mapping allows the problem of finding the center of mass on $\mathbb{S}^2_R$ to be reduced to calculating it on the one-dimensional sphere $\mathbb{S}^1_R$. When considering the stereographic projection of $\mathbb{S}^1_R$ onto the real axis, a point $P(x, y)$ on $\mathbb{S}^1_R$ corresponds to a point u on the real axis, where $u = \frac{Rx}{R-y}$ and $P(0, R) = \infty$. The inverse projection is given by*

$$P^{-1}(u) = \begin{pmatrix} \frac{2R^2 u}{u^2+R^2} \\ \frac{R(u^2-R^2)}{u^2+R^2} \end{pmatrix}.$$

Proof. The proof involves demonstrating the isometry that maps the points on $\mathbb{S}^2_R$ to $\mathbb{S}^1_R$. First, we consider two rotations: one that aligns the axis passing through the two points with the z-axis, and another that rotates the points to the xy-plane. This process does not alter the relative distances between points, preserving the center of mass due to the invariance under isometries.

Next, we consider the stereographic projection from $\mathbb{S}^1_R$ to the real line. A point $P(x, y)$ on $\mathbb{S}^1_R$ is mapped to a point u on the real axis using the formula $u = \frac{Rx}{R-y}$. The inverse mapping, $P^{-1}(u)$, is necessary to retrieve the original points on the sphere from their projections.

By applying these transformations, the calculation of the center of mass on $\mathbb{S}^2_R$ is effectively reduced to a simpler problem on $\mathbb{S}^1_R$ and further to a calculation on the real line via stereographic projection. □

7.1. Arc Length from the South Pole

Theorem 10. *Let $\mathbb{S}^1_R$ be a sphere of radius R. The arc length s, extending from the south pole to a specific point (x, y) on $\mathbb{S}^1_R$, whose stereographic projection is u, is calculated by*

$$s = 2R \arctan\Big(\frac{u}{R}\Big).$$

More generally, the arc length s from point $Q_1(x_1, y_1)$ to point $Q_2(x_2, y_2)$ on $\mathbb{S}^1_R$, whose stereographic projections are u_1 and u_2, respectively, (with $u_1 < u_2$), is given by

$$s = 2R\Big(\arctan\Big(\frac{u_2}{R}\Big) - \arctan\Big(\frac{u_1}{R}\Big)\Big).$$

Proof. For the first case, consider the integral representing the arc length from the south pole to a point whose stereographic projection is u:

$$s = 2R^2 \int_0^u \frac{1}{t^2 + R^2} dt.$$

Using the definite integral of the arctangent function, we obtain

$$s = 2R^2 \left[\frac{1}{R} \arctan\left(\frac{t}{R}\right)\right]_0^u = 2R\Big[\arctan\Big(\frac{u}{R}\Big) - \arctan(0)\Big] = 2R \arctan\Big(\frac{u}{R}\Big).$$

For the general case, the arc length between two points Q_1 and Q_2 is calculated by considering the difference between the arc lengths from the south pole to each point:

$$s = 2R\Big(\arctan\Big(\frac{u_2}{R}\Big) - \arctan\Big(\frac{u_1}{R}\Big)\Big).$$

This is directly deduced from the additive property of the arc length and the arctangent function, providing a consistent way to calculate the distance along the sphere between any two given points. □

7.2. Center of Mass

Theorem 11. *Consider two masses $m_k, k = 1, 2$, located at points $Q_k, k = 1, 2$, respectively. Let $Q_c(x_c, y_c)$ be the point that satisfies the lever rule on the sphere $m_1 s_1 = m_2 s_2$. Then, the following equality holds:*

$$\arctan\Big(\frac{u_c}{R}\Big) = \frac{1}{m_1 + m_2}\Big(m_1 \arctan\Big(\frac{u_1}{R}\Big) + m_2 \arctan\Big(\frac{u_2}{R}\Big)\Big). \tag{27}$$

Proof. Given the lever rule on the sphere $m_1 s_1 = m_2 s_2$, we can express this relationship as

$$2Rm_1\Big(\arctan\Big(\frac{u_c}{R}\Big) - \arctan\Big(\frac{u_1}{R}\Big)\Big) = 2Rm_2\Big(\arctan\Big(\frac{u_2}{R}\Big) - \arctan\Big(\frac{u_c}{R}\Big)\Big).$$

By simplifying this equation, we isolate $\arctan\big(\frac{u_c}{R}\big)$:

$$2Rm_1 \arctan\Big(\frac{u_c}{R}\Big) - 2Rm_1 \arctan\Big(\frac{u_1}{R}\Big) = 2Rm_2 \arctan\Big(\frac{u_2}{R}\Big) - 2Rm_2 \arctan\Big(\frac{u_c}{R}\Big).$$

$$2R(m_1 + m_2) \arctan\Big(\frac{u_c}{R}\Big) = 2Rm_1 \arctan\Big(\frac{u_1}{R}\Big) + 2Rm_2 \arctan\Big(\frac{u_2}{R}\Big).$$

$$\arctan\Big(\frac{u_c}{R}\Big) = \frac{1}{m_1 + m_2}\Big(m_1 \arctan\Big(\frac{u_1}{R}\Big) + m_2 \arctan\Big(\frac{u_2}{R}\Big)\Big).$$

This concludes the proof, demonstrating that the point $Q_c(x_c, y_c)$ indeed satisfies the lever rule with respect to the given masses and positions on the sphere. □

Theorem 12. *Consider, n point masses $m_k, k = 1, \ldots, n$ situated at the coordinates (x_k, y_k, z_k), $k = 1, \ldots, n$ on $\mathbb{S}^2_R$, all lying on the same geodesic. Further, let their stereographic projections be $w_1, w_2, \ldots, w_n$ in $\mathbb{C}$. Consider the equation*

$$\arctan\Big(\frac{w_c}{R}\Big) = \frac{1}{m}\sum_{k=1}^{n} m_k \arctan\Big(\frac{w_k}{R}\Big),$$

If we multiply both sides by R and take the limit as $R \to \infty$, we obtain

$$w_c = \frac{1}{m}\sum_{k=1}^{n} m_k w_k. \tag{28}$$

This matches the expression for the center of mass in the Euclidean complex plane, specifically within the complex plane (or $\mathbb{R}^2$), characterized by a Euclidean metric and null curvature.

Proof. In a broader context, consider n point masses $m_k, k = 1, \ldots, n$ situated at the coordinates $(x_k, y_k, z_k), k = 1, \ldots, n$ on $\mathbb{S}^2_R$, all lying on the same geodesic. Let their stereographic projections be $w_1, w_2, \ldots, w_n$ in $\mathbb{C}$. Then, if w_c is their spherical center of mass, the following relationship is satisfied:

$$\arctan\Big(\frac{w_c}{R}\Big) = \frac{1}{m}\sum_{k=1}^{n} m_k \arctan\Big(\frac{w_k}{R}\Big),$$

where $m = \sum_{k=1}^{n} m_k$.

Consider the equation given in the theorem. We multiply both sides by R to facilitate the application of L'Hôpital's rule:

$$R \cdot \arctan\Big(\frac{w_c}{R}\Big) = \frac{R}{m}\sum_{k=1}^{n} m_k \arctan\Big(\frac{w_k}{R}\Big).$$

As $R \to \infty$, we encounter an indeterminate form $\infty \cdot 0$ on both sides of the equation. To resolve this, we apply L'Hôpital's rule by differentiating the numerator and the denominator with respect to R. This involves computing the derivative of $\arctan\big(\frac{w}{R}\big)$ with respect to R, which gives $-\frac{w}{R^2+w^2}$.

Applying L'Hôpital's rule, we have

$$\lim_{R\to\infty} \frac{\arctan\big(\frac{w_c}{R}\big)}{\frac{1}{R}} = \frac{1}{m}\sum_{k=1}^{n} m_k \lim_{R\to\infty} \frac{\arctan\big(\frac{w_k}{R}\big)}{\frac{1}{R}}.$$

After applying the rule and simplifying, we find

$$\lim_{R\to\infty} \frac{R^2}{R^2 + w_c^2} w_c = \frac{1}{m} \sum_{k=1}^{n} m_k \lim_{R\to\infty} \frac{R^2}{R^2 + w_k^2} w_k,$$

which simplifies to the desired result as $R \to \infty$:

$$w_c = \frac{1}{m} \sum_{k=1}^{n} m_k w_k,$$

matching the expression for the center of mass in the Euclidean complex plane. □

8. Conclusions

The document focuses on the relationship between spherical geometry and the n-body problem on a two-dimensional conformal sphere, M_R^2. The main conclusions drawn from the results, theorems, and corollaries are summarized below:

1. Radius–mass relationship: A specific condition related to the radius–mass relationship of the particles is established. Under this condition, two antipodal point particles with positive mass move unrestrictedly in a state of relative equilibrium along a geodesic associated with the canonical Killing vector field in M_R^2.
2. Relative equilibrium: The exploration of how variations in the sphere's radius and the particles' masses affect the behavior of relative equilibrium provides a deeper understanding of the relationships between the system's parameters and its dynamics.
3. Geodesic movement: It is concluded that an even number of point particles, with pairwise conjugated positions and arranged in a regular n-gon with equal masses, move freely on a geodesic with particular velocities, behaving as a relative equilibrium.
4. Center of mass on the sphere: An approach to determining the center of mass on a two-dimensional sphere is discussed, using stereographic projection and relating it to the calculation of the center of mass on the one-dimensional sphere S_R^1.
5. Arc length: A method is provided to calculate the arc length from the south pole to a specific point on S_R^1, crucial for understanding the geometry involved in the n-body problem on a sphere.

Author Contributions: Writing—review and editing, R.D.O.O., A.M.M.R. and I.O.d.J. All authors have read and agreed to the published version of the manuscript.

Funding: This research was funded by the Universidad de Cartagena, grant number 014-2022. The APC was funded by the Universidad de Cartagena.

Institutional Review Board Statement: Not applicable.

Informed Consent Statement: Not applicable.

Data Availability Statement: This article does not rely on the analysis of numerical or experimental datasets, given its focus on theoretical mathematical research. Therefore, no new data were created or analyzed during the study.

Acknowledgments: This work was supported by the Universidad de Cartagena. We dedicate this work to the memory of our dear friend and co-author, Pedro Pablo Ortega Palencia, who worked hard on solving problems of celestial mechanics with curvature [2,3] and played a crucial role in the publication of this work.

Conflicts of Interest: The authors declare no conflicts of interest. Our study is purely theoretical and does not involve any empirical data that could potentially lead to conflicts related to data collection, analysis, or interpretation. We have maintained complete academic integrity and impartiality throughout the research process. Our findings and conclusions are presented without any undue influence from personal interests or funding sources.

References

1. Borisov, A.V.; García-Naranjo, L.; Mamaev, I.S.; Montaldi, J. Reduction and relative equilibria for the two-body on spaces of constant curvature. *Celest. Mech. Dyn. Astr.* **2018**, *130*, 43. [CrossRef]
2. Ortega-Palencia, P.P.; Reyes-Victoria, J.G. On certain Möbius type solutions for the n-body problem in a positive space form. *arXiv* **2015**, arXiv:1508.03209.
3. Palencia, P.P.O.; Ortiz, R.D.O.; Ramirez, A.M.M. Hyperbolic center of mass for a system of particles in a two-dimensional space with constant negative curvature: An application to the curved 2-body problem. *Mathematics* **2021**, *9*, 531. [CrossRef]
4. Diacu, F.; Pérez-Chavela, E.; Santoprete, M. The n-body problem in spaces of curvature constant. *arXiv* **2008**, arXiv:0807.1747.
5. Abraham, R.; Marsden, J. *Foundations of Mechanics*, 2nd ed.; Addison-Wesley Pub. Co.: Redwood City, CA, USA, 1987.
6. Ortega-Palencia, P.P.; Ortiz, R.D.; Reyes-Victoria, J.G. A simple expression for the center of mass of a system of particles in a two-dimensional space with constant positive curvature. *J. Eng. Appl. Sci.* **2019**, *14*, 9603–9607. [CrossRef]
7. Ortega-Palencia, P.P.; Reyes-Victoria, J.G. Conjugate Equilibrium Solutions for the 2–Body Problem in the Two Dimensional Sphere $\mathbb{M}^2_R$ for Equal Masses. *arXiv* **2019**, arXiv:1908.06011.
8. Pérez-Chavela, E.; Reyes-Victoria, J.G. An intrinsic approach in the curved n-body problem. The positive curvature case. *Trans. Am. Math. Soc.* **2012**, *364*, 3805–3827. [CrossRef]
9. Pérez-Chavela, E.; Sánchez-Cerritos, J.M. Regularization of the restricted (n+1)(n+1)-body problem on curved spaces. *Astrophys. Space Sci.* **2019**, *364*, 170. [CrossRef]
10. Sánchez-Cerritos, J.M.; Pérez-Chavela, E. Hyperbolic regularization of the restricted three–body problem on curved spaces. *Anal. Math. Phys.* **2022**, *12*, 23. [CrossRef]
11. Álvarez-Ramírez, M.; García, A.; Meléndez, J.; Reyes-Victoria, J.G. The three-body problem and equivariant Riemannian geometry. *J. Math. Phys.* **2017**, *58*, 083507. [CrossRef]
12. Montgomery, R. Fitting hyperbolic pants to a three-body problem. *Ergodic Theory Dyn. Syst.* **2005**, *25*, 921–948. [CrossRef]
13. Kozlov, V.; O'Harin, A. Kepler's problem in constant curvature spaces. *Celest. Mech. Dyn. Astr.* **1992**, *54*, 393–399. [CrossRef]
14. Dubrovine, B.; Fomenko, A.; Novikov, P. *Modern Geometry, Methods and Applications, Vol. I, II, and III*; Springer: Berlin/Heidelberg, Germany, 1984.
15. Farkas, H.M.; Kra, I. *Riemann Surfaces*; Springer: Berlin/Heidelberg, Germany, 1988.
16. Diacu, F.; Pérez-Chavela, E.; Reyes, J.G. An intrinsic approach in the curved n-body problem. The negative case. *J. Differ. Equ.* **2012**, *252*, 4529–4562. [CrossRef]
17. Borisov, A.V.; Mamaev, I.S.; Kilin, A.A. Two-body problem on a sphere. Reduction, stochasticity, periodic orbits. *Regul. Chaotic Dyn.* **2004**, *9*, 265–279. [CrossRef]